

Supporting Information

Excitation wavelength dependence of the charge separation pathways in tetraphorphyrin-naphthalene diimide pentads

Diego Villamaina,^a Melissa M. Kelson,^b Sheshanath V. Bhosale,^b and Eric Vauthey^{a*}

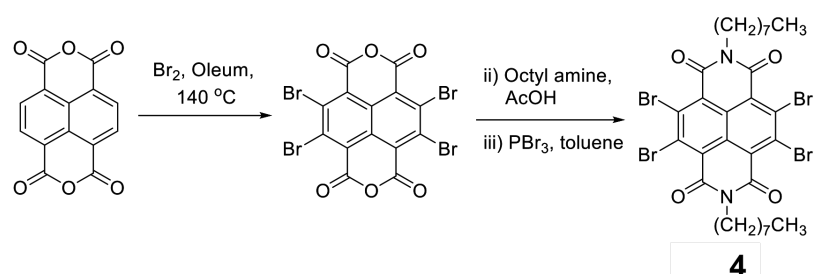
a) Department of Physical Chemistry, University of Geneva, 30 Quai Ernest-Ansermet, CH-1211 Geneva 4, Switzerland

b) School of Applied Sciences, RMIT University, GPO Box 2476V, Melbourne, Vic. 3001, Australia

Synthesis of arrays 1 and 2

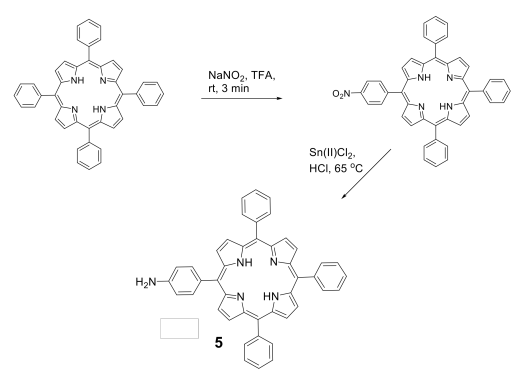
Naphthalenetetracarboxy dianhydride, octylamine, acetic acid (AcOH), pyrrole, benzaldehyde, boron trifluoride etherate ($\text{BF}_3 \cdot \text{O}(\text{Et})_2$), 2,3-Dichloro-5,6-dicyano-1,4-benzoquinone (DDQ), bromine (Br_2), dimethyl formamide (DMF), toluene, chloroform (CHCl_3), chloroform-d (CDCl_3), methanol (MeOH) and dichloromethane (DCM), zinc acetate ($\text{Zn}(\text{OAc})_2 \cdot 2\text{H}_2\text{O}$) were purchased from Aldrich and used without purification, unless otherwise specified. UV-vis absorption spectra were recorded on a Cary-50 UV-Vis spectrophotometer. ^1H NMR, ^{13}C -NMR spectra were recorded on a Bruker spectrometer using CDCl_3 as solvent and tetramethylsilane (TMS) as an internal standard. The solvents for spectroscopic studies were of spectroscopic grade and used as without further purification.

1) Preparation of 2,3,6,7-tetrabromo-dioctyl-naphthalene diimide (4):



Compound 4 was prepared following literature procedure starting from naphthalene dianhydride (NDA) in three steps:^{S1} 1) the preparation of 2,3,6,7-tetrabromonaphthalene dianhydride (Br_4NDA) by treatment of NDA with Br_2 (5.3 equiv) in a mixture of sulfuric acid and oleum ($v:v$, 4:1) at 140°C with 96% yields; 2) the reaction of Br_4NDA with octyl amine in acetic acid; 3) the reaction of the intermediate with excess PBr_3 in refluxing toluene for 12 h giving 4 in 31.4% yield. All spectroscopic data match literature.^{S1}

2) Preparation of 5-(4-aminophenyl)-10,15,20-triphenylporphyrin (5):

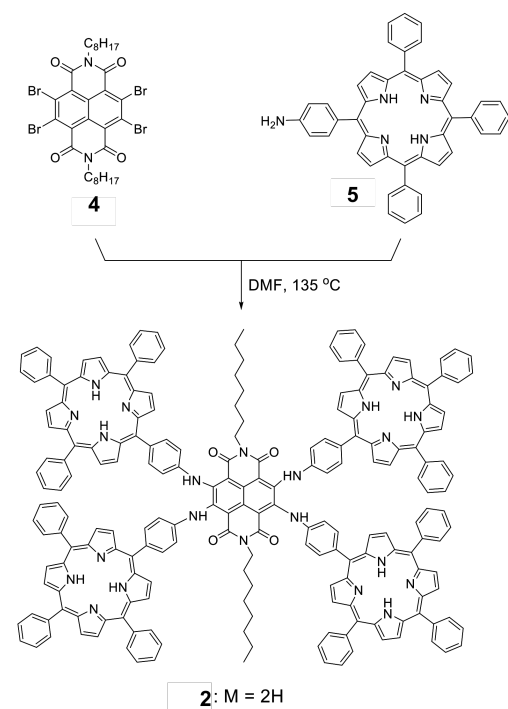


5 was prepared in two steps following literature:^{S2} 1) nitration of 5,10,15,20-tetraphenylporphyrin (100 mg) with NaNO_2 (1.8 equiv) in TFA (5.5 mL) stirred for 3 minutes at room temperature; 2) quenching of the reaction with water (100 mL) and extraction with chloroform (25 mL). The

organic layers were washed once with saturated aqueous NaHCO_3 and followed by washing once with brine, and dried over anhydrous Na_2SO_4 . Nitro-porphyrin was purified by column chromatography eluting with chloroform giving 85 mg of 5-(4-nitrophenyl)-10,15,20-triphenylporphyrin as a yellowish solid. The reduction of meso-(4-nitrophenyl)phenylporphyrin was carried out by tin chloride. Typically, 50 mg of mono-nitro porphyrin was dissolved in hydrochloric acid (10 mL) then Sn(II)Cl_2 (200 mg) was added over 15 minutes. The final mixture was heated to 65°C for 1 h under argon. Completion of the reactions was confirmed by TLC, water was added, and the aqueous solution was then neutralized with ammonium hydroxide until pH 8. The aqueous solution was extracted with chloroform (4x50mL). The organic

layer was then concentrated under vacuum and the residue purified on a plug of silica gel using chloroform as an eluent to give 23 mg of compound **5**. The spectroscopic characterisation of **5** is in good agreement with literature. ⁸² ¹H NMR (CDCl₃) δ ppm: -2.75 (br, 2H), 4.02 (s, 2H), 7.07 (d, *J* = 8.9 Hz, 2H), 7.75 (m, 9H), 7.98 (d, *J* = 8.9 Hz, 2H), 8.20 (m, 6H), 8.84 (s, 6H), 8.96 (s, 2H). Anal. Calcd for C₄₄H₃₁N₅: C, 83.92; H, 4.96; N, 11.12. Found: C, 83.87; H, 4.95; N, 10.98. Maldi (mass) m/z for C₄₄H₃₁N₅ 629.7670 (calc.), 629.7589.

3) Synthesis of Fb(TPP)₄NDI (2):

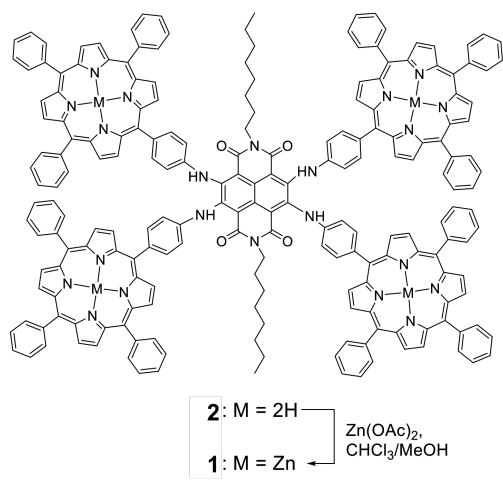


A mixture of 2,3,6,7-tetrabromo-dioctyl-naphthalene diimide **4** (50 mg, 6.20x10⁻⁵ M) and 5-(4-Aminophenyl)-10,15,20-triphenylporphyrin **5** (187 mg, 2.9x10⁻⁴ M) in dry DMF (2.5 mL) was heated at 135 °C for 12 h, and the completion of the reaction was monitored by TLC. After completion, DMF was evaporated and the residual was purified by column chromatography on a flash silica column, eluted with chloroform. **2** (85 mg, 45%) was obtained as dark purple crystals. Mp > 300 °C. ¹H NMR (CDCl₃, 400 MHz) δ 12.47 (s, 4H, core-NH), 9.24-9.23 (d, *J* = 9.0

Hz, 8H, b-pyrrolic), 8.90-8.89 (d, *J* = 8.7 Hz, 8H, b-pyrrolic), 8.87-8.86 (d, *J* = 8.7 Hz, 8H, b-pyrrolic), 8.81-8.80 (d, *J* = 9.0 Hz, 8H, b-pyrrolic), 8.27-8.25 (d, *J* = 7.6 Hz, 8H), 8.19-8.17 (d, *J* = 7.6 Hz, 8H), 8.08 (br, 16H), 7.77-7.69 (m, 12H), 7.55-7.51 (br, 24H), 7.47-7.45 (d, *J* = 8.2 Hz, 8H), 4.51-4.48 (t, *J* = 8.2 Hz, 4H), 1.68-1.63 (m, 4H), 1.39-1.25 (m, 20), 0.90-0.88 (t, *J* = 7.2 Hz, 6H), -2.89 (br, s, 8H, NH, porphyrin core). ¹³C NMR (CDCl₃, 125 MHz) δ 166.22, 150.46, 150.20, 150.18, 150.15, 142.81, 142.69, 138.94, 134.38, 134.27, 132.02, 131.92, 131.47, 127.30, 126.51, 126.37, 124.46, 121.10, 121.05, 120.98, 118.71, 41.31, 131.92, 31.86, 29.69, 29.65, 29.41, 29.19, 22.68, 22.65, 14.09. FT-IR (KBr, Cm⁻¹) ν 3389, 3331, 2987, 2969, 2878, 1714, 1665, 1507, 1483, 1438, 1374, 1287, 1173, 1157, 1013, 918, 791, 854. HRMS (ESI): calcd. for C₂₀₆H₁₅₄N₂₂O₄: m/z 3001.5720; found 3001.5721. Elemental analysis

calcd (%) for $C_{206}H_{154}N_{22}O_4$: C, 82.43; H, 5.17; N, 10.27; found C, 82.38; H, 5.04; N, 10.18.

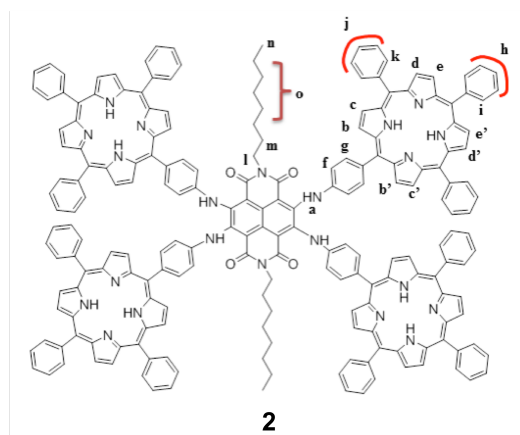
4) Synthesis of $Fb(TPP)_4NDI$ (2):



To a solution of $Fb(TPP)_4NDI$ (2) (50 mg) in $CHCl_3$ (10 mL), $Zn(OAc)_2 \cdot 2H_2O$ (80 mg, excess) dissolved in $MeOH$ (1 mL) was added. The mixture was stirred overnight at room temperature. The mixture was then washed with water and dried over anhydrous sodium sulfate. The compound was purified over a silica gel column using $CHCl_3$ as the eluent and 51 mg of 1 as purple solid were obtained (94% yield). $Mp > 300$ °C; 1H

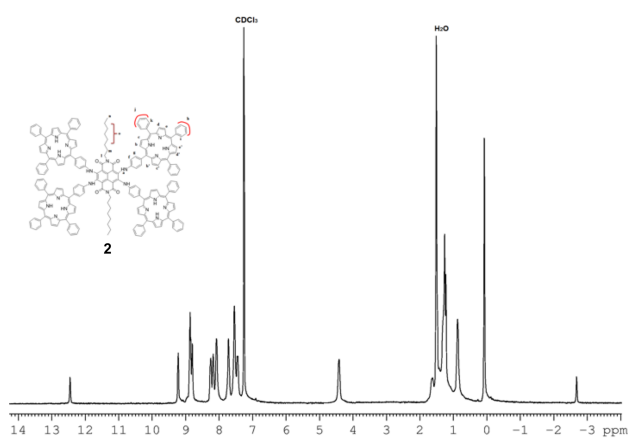
NMR ($CDCl_3$, 400 MHz) δ 12.46 (s, 4H, core-NH), 9.23-9.22 (d, $J = 9.0$ Hz, 8H, b-pyrrolic), 8.89-8.87 (d, $J = 8.7$ Hz, 8H, b-pyrrolic), 8.86-8.85 (d, $J = 8.7$ Hz, 8H, b-pyrrolic), 8.82-8.80 (d, $J = 9.0$ Hz, 8H, b-pyrrolic), 8.27-8.25 (d, $J = 7.6$ Hz, 8H), 8.19-8.18 (d, $J = 7.6$ Hz, 8H), 8.09 (br, 16H), 7.76-7.71 (m, 12H), 7.69-7.55 (br, 24H), 7.46-7.44 (d, $J = 8.2$ Hz, 8H), 4.49-4.46 (t, $J = 8.2$ Hz, 4H), 1.66-1.62 (m, 4H), 1.37-1.18 (m, 20), 0.89-0.88 (t, $J = 7.2$ Hz, 6H). ^{13}C NMR ($CDCl_3$, 125 MHz) δ 166.21, 150.44, 150.16, 150.13, 142.89, 142.77, 138.92, 137.87, 134.41, 134.29, 131.87, 127.27, 126.48, 126.35, 121.03, 120.98, 120.92, 119.49, 118.68, 109.31, 31.86, 29.69, 29.60, 29.47, 29.42, 27.55, 22.64, 14.09. FT-IR (KBr, Cm^{-1}) ν 3393, 3329, 2978, 2965, 2873, 1717, 1666, 1503, 1481, 1441, 1378, 1287, 1178, 1152, 1019, 913, 797, 855. HRMS (ESI): calcd. for $C_{206}H_{146}N_{22}O_4Zn_4$: m/z 3255.0284; found 3255.0173. Elemental analysis calcd (%) for $C_{206}H_{146}N_{22}O_4Zn_4$: C, 76.01; H, 4.52; N, 9.47; found C, 75.98; H, 4.49; N, 9.34.

5) Detailed characterisation of 1 and 2:

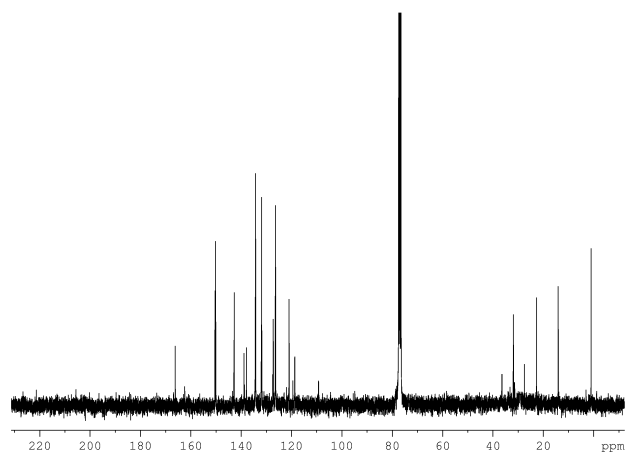


δ 12.47 (s, 4H, core-NH), 9.24-9.23 (d, J = 9.0 Hz, 8H, b-pyrrolic-**b**), 8.90-8.89 (d, J = 8.7 Hz, 8H, b-pyrrolic, **d**), 8.87-8.86 (d, J = 8.7 Hz, 8H, b-pyrrolic, **e**), 8.81-8.80 (d, J = 9.0 Hz, 8H, b-pyrrolic, **c**), 8.27-8.25 (d, J = 7.6 Hz, 8H, **f**), 8.19-8.17 (d, J = 7.6 Hz, 8H, **k**), 8.08 (br, 16H, **g**), 7.77-7.69 (m, 12H, **h**), 7.55-7.51 (br, 24H, **j**), 7.47-7.45 (d, J = 8.2 Hz, 8H, **i**), 4.51-4.48 (t, J = 8.2 Hz, 4H, **l**), 1.68-1.63 (m, 4H, m), 1.39-1.25 (m, 20, o), 0.88-0.84 (t, J = 7.2 Hz 6H, n), -2.89 (br, s, 8H, NH, porphyrin core)

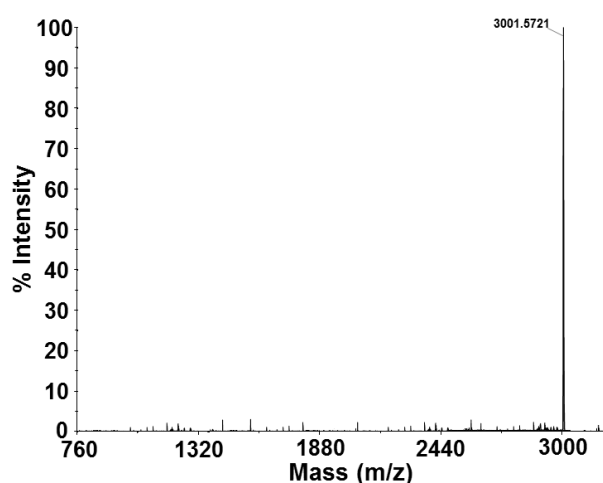
^1H NMR of **Fb(TPP)₄NDI** (**2**):



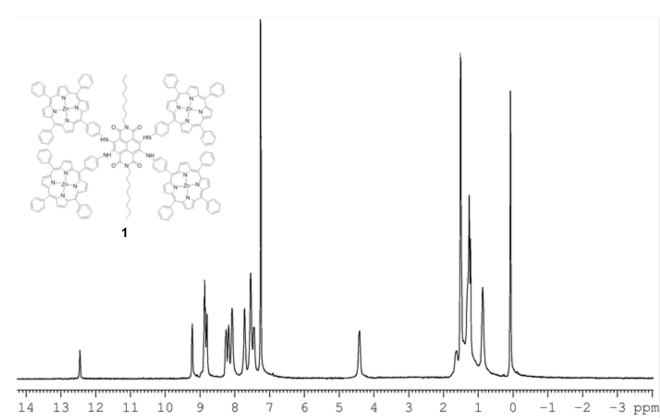
^{13}C NMR of **Fb(TPP)₄NDI** (**2**):



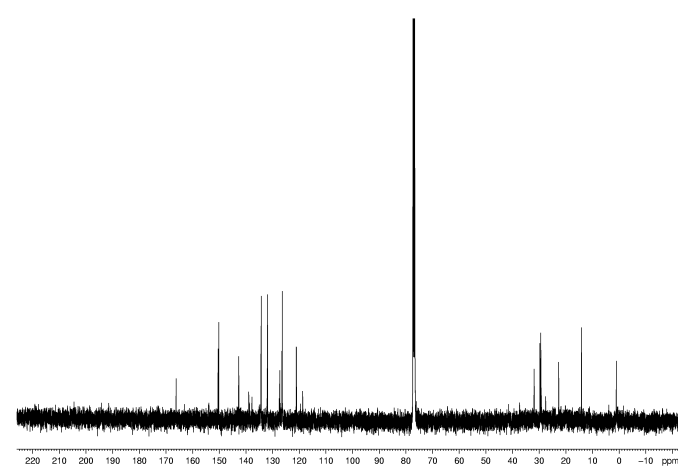
HRMS of *Fb*(TPP)₄NDI (2):



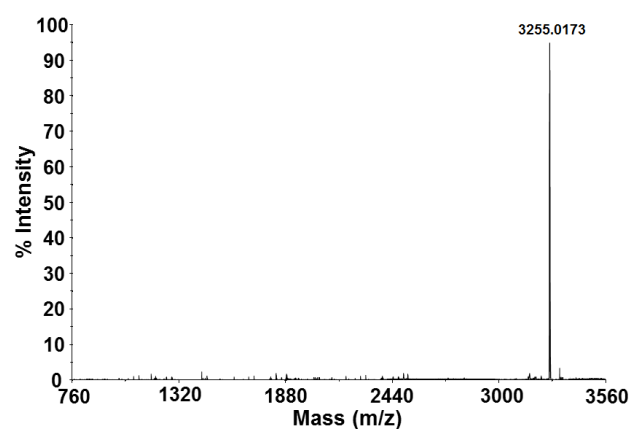
¹H NMR of Zn(TPP)₄NDI (1):



¹³C NMR of Zn(TPP)₄NDI (1):



HRMS of $Zn(TPP)_4NDI$ (**1**):



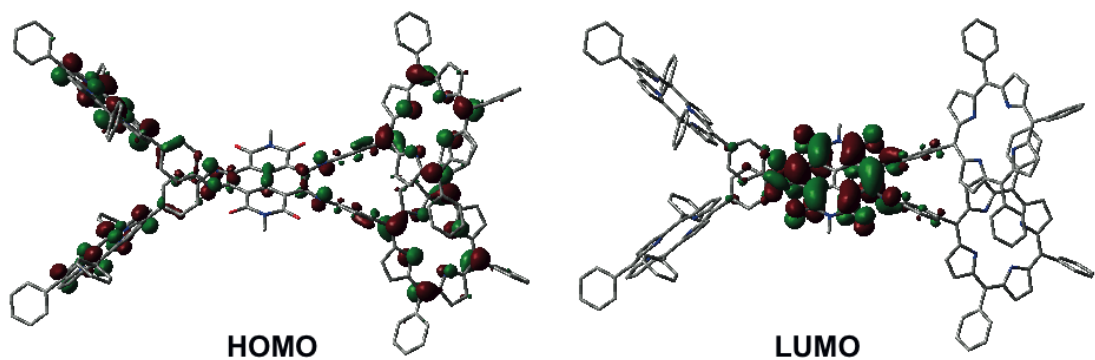


Figure S1: optimised geometry of **2** and frontier molecular orbitals computed at the B3LYP/6-31G* level of theory (the H atoms are omitted for better visibility, the calculations have been done with methyl instead of octyl substituents on the imide N atoms).

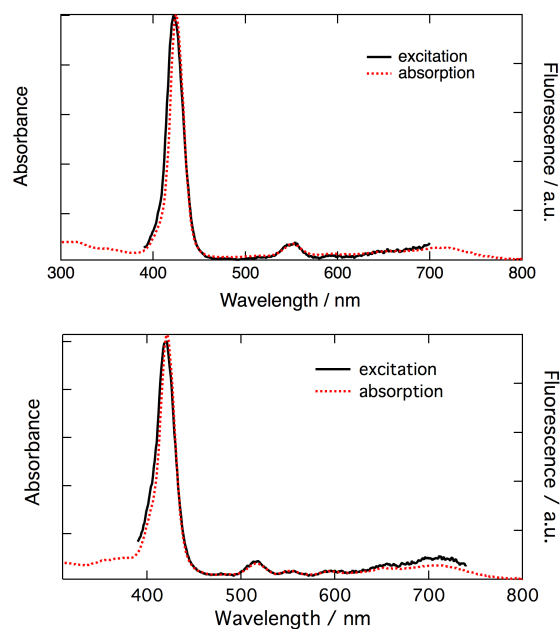


Figure S2: comparison of the fluorescence excitation spectra of **1** (top) and **2** (bottom) measured at 760 nm in toluene.

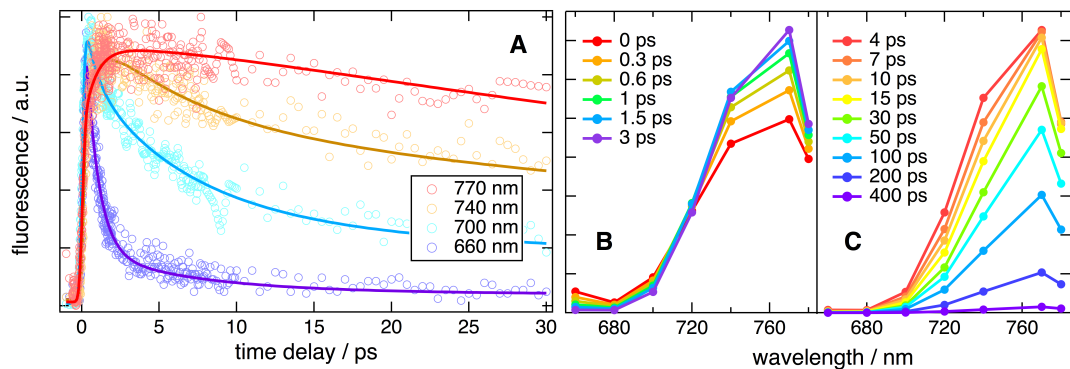


Figure S3: A) time profiles of the fluorescence intensity measured at several wavelengths upon $L_B \leftarrow S_0$ excitation of **1** in toluene and best fit obtained from a global multiexponential analysis (solid lines); B,C) reconstructed time-resolved emission spectra.

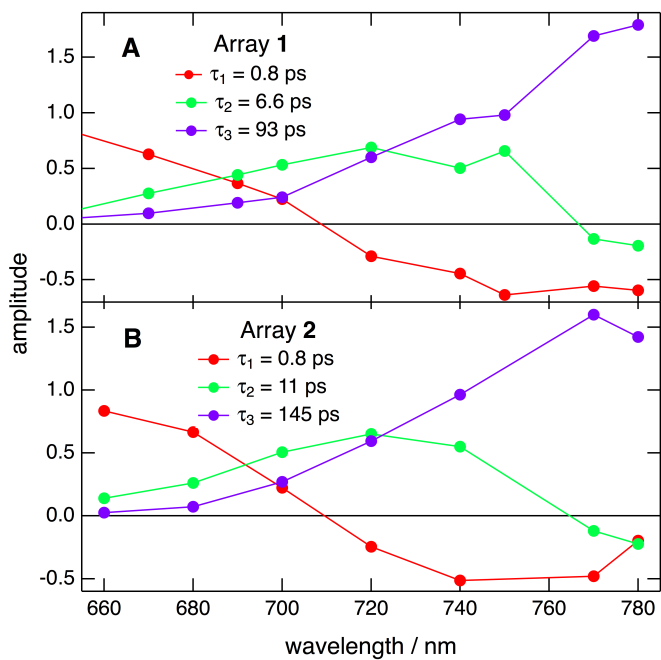


Figure S4: Decay-associated spectra obtained from a multiexponential global analysis of the fluorescence time profiles measured with array **1** (A) and array **2** (B) in toluene.

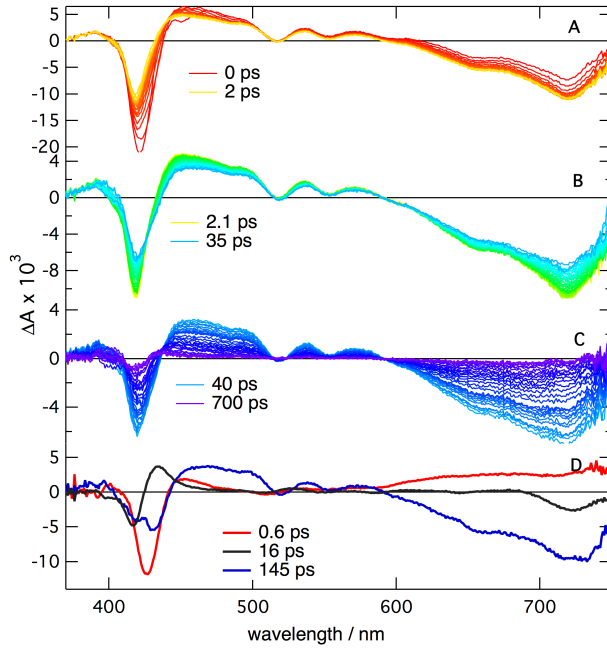


Figure S5: (A-C) transient absorption spectra measured at several time delays after $L_B \leftarrow S_0$ excitation of **2** in toluene, and (D) decay-associated difference spectra obtained from a global multiexponential analysis.

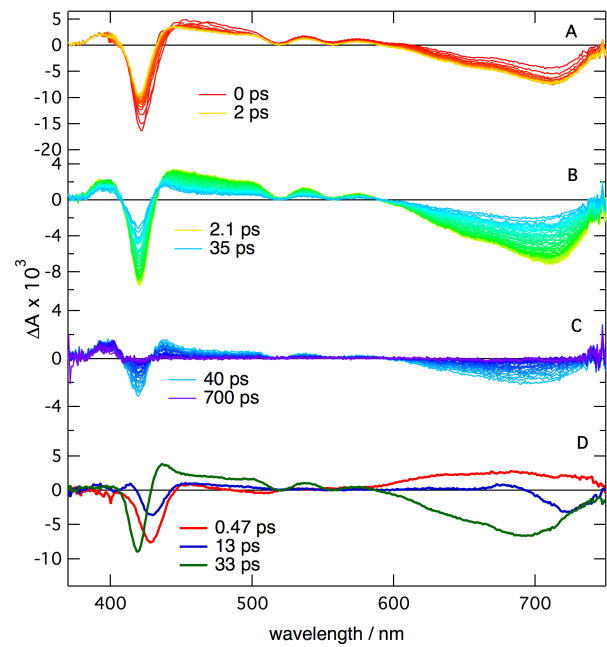


Figure S6: (A-C) transient absorption spectra measured at several time delays after $L_B \leftarrow S_0$ excitation of **2** in benzonitrile, and (D) decay-associated difference spectra obtained from a global multiexponential analysis.

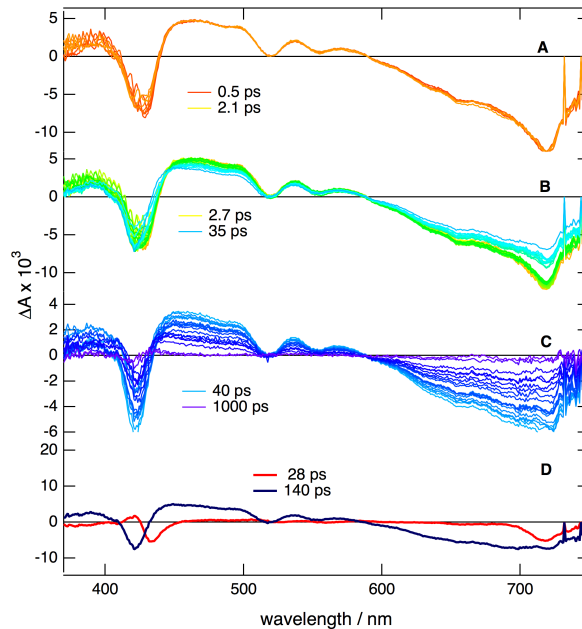


Figure S7: (A-C) transient absorption spectra measured at several time delays after $S_1 \leftarrow S_0$ excitation of **2** in toluene, and (D) decay-associated difference spectra obtained from a global multiexponential analysis.

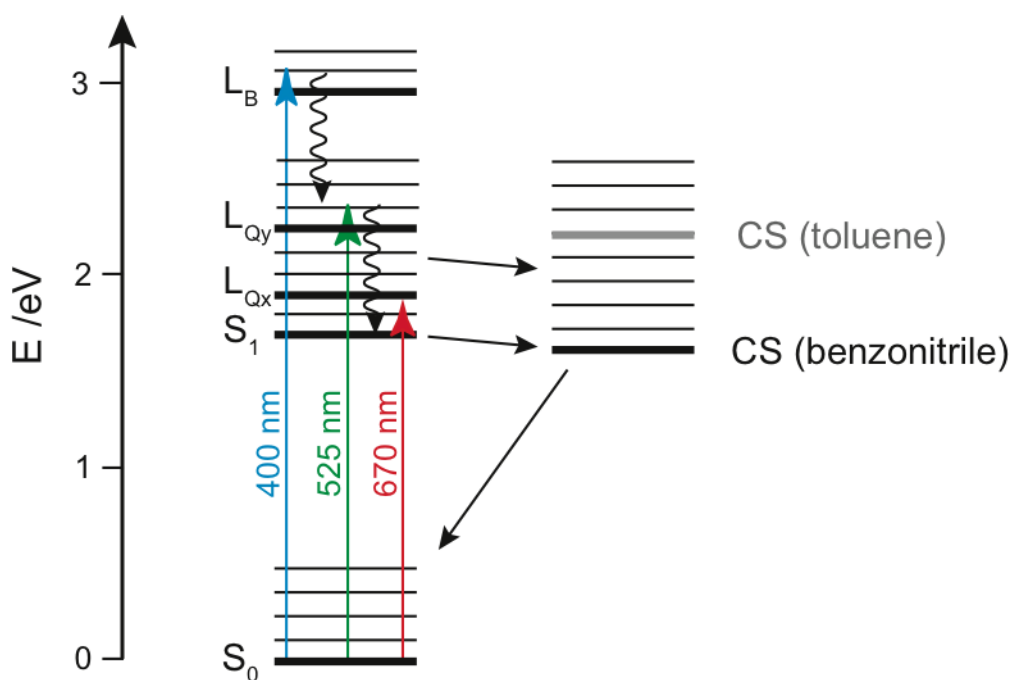


Figure S8: energy-level scheme of **2**.

Calculation of the excitation energy hopping (EEH) rate constants

According to Förster theory, the EET rate constant, in ps^{-1} , can be expressed as:^{S3}

$$k_{\text{EEH}(T)} = 1.18(\text{ps}^{-1}\text{cm}) \cdot |V_{dd}|^2 \Theta \quad (\text{S1})$$

where V_{dd} is the interaction energy between the transition dipole moments of the energy donor and acceptor and Θ is the spectral overlap integral, obtained from the area-normalized emission and absorption bands of the donor and acceptor, respectively, represented on a wavenumber scale.

The dipole-dipole energy, V_{dd} , in cm^{-1} between two chromophores with a transition dipole, $\vec{\mu}_d$ and $\vec{\mu}_a$ (in D), where d and a are the energy donor and acceptor, respectively, at a distance $|\vec{r}_{da}| = r_{da}$ (in nm) can be calculated as:

$$V_{dd} = 5.04 \frac{|\vec{\mu}_d| |\vec{\mu}_a| f_L^2}{\epsilon_{op} r_{da}^3} \kappa \quad (\text{S2})$$

where $\epsilon_{op} \approx n^2$ is the dielectric constant at optical frequencies, n is the refractive index, $f_L = (\epsilon_{op} + 2)/3$ the Lorentz local field correction factor, and κ the orientational factor:

$$\kappa = \cos \beta_{da} - 3 \cos \beta_d \cos \beta_a \quad (\text{S3})$$

with β_{da} , the angle between $\vec{\mu}_d$ and $\vec{\mu}_a$, and β_d and β_a the angles between the dipoles and \vec{r}_{da} .

The B and Q states of ZnP are doubly degenerate with two perpendicular transition dipole moments ($\vec{\mu}_x$ and $\vec{\mu}_y$) located in the porphyrin plane (planar transition dipole).

Therefore, the EEH rate constant between two ZnP units is the sum of four contributions:

$$k_{\text{EEH}} = k_{xx} + k_{yy} + k_{xy} + k_{yx} \quad (\text{S4})$$

We consider only the EEH between two adjacent ZnP units of the pentad, i.e. in 2-3 or 6-7 position. We place the x and y axes parallel and perpendicular to the axis connecting the ZnP to the c-NDI. In the optimised geometry of array **1**, the angle between $\vec{\mu}_x(d)$ and $\vec{\mu}_y(a)$ is always 90 deg, that between $\vec{\mu}_x(d)$ and $\vec{\mu}_x(a)$ is 31.75 deg and that between $\vec{\mu}_y(d)$ and $\vec{\mu}_y(a)$ is 0 deg.

These values can be used to calculate V_{xx} and V_{yy} . For calculating k_{EEH} , the sum of the square values is used:

$$V_{dd}^2 = V_{xx}^2 + V_{yy}^2 \quad (S5)$$

The interaction energy discussed in the main text corresponds to:

$$|V_{dd}| = \sqrt{V_{xx}^2 + V_{yy}^2} \quad (S6)$$

In all cases, a refractive index of $n=1.5$ was used.

The following parameters have been used for the calculation of the various EEH rate constants:

1) L_B EEH between two adjacent ZnP units:

$$|\vec{\mu}_x| = |\vec{\mu}_y| = 7.8 \text{ D}, r_{da} = 1.17 \text{ nm}$$

$$|V_{xx}| = 172 \text{ cm}^{-1}, |V_{yy}| = 184 \text{ cm}^{-1}, |V_{dd}| = 252 \text{ cm}^{-1}.$$

$$\text{Spectral overlap integral: } \Theta = 5.7 \cdot 10^{-4} \text{ cm}^{-4}$$

$$k_{EEH} = (0.025 \text{ ps})^{-1}$$

2) L_Q EEH between two adjacent ZnP units:

$$|\vec{\mu}_x| = |\vec{\mu}_y| = 2.25 \text{ D}, r_{da} = 1.17 \text{ nm}$$

$$|V_{xx}| = 14.3 \text{ cm}^{-1}, |V_{yy}| = 15.3 \text{ cm}^{-1}, |V_{dd}| = 21 \text{ cm}^{-1}.$$

$$\text{Spectral overlap integral: } \Theta = 5.2 \cdot 10^{-5} \text{ cm}^{-4}$$

$$k_{EEH} = (36 \text{ ps})^{-1}$$

The situation is different for EEH between FbP units in **2** as the Q states are not longer degenerated but split into Q_y and Q_x states, the latter being the lowest one. Because of the spectral overlap and the extremely fast $Q_y \rightarrow Q_x$ relaxation, only Q_x EEH needs to be considered. Because each FbP in a porphyrin pair can exist in two tautomeric forms, four possible mutual orientations of the $Q_x \leftarrow S_0$ transition dipoles, hence four EEH paths, need to be considered:

1) $\vec{\mu}_1(d)$ to $\vec{\mu}_1(a)$; 2) $\vec{\mu}_1(d)$ to $\vec{\mu}_2(a)$; 3) $\vec{\mu}_2(d)$ to $\vec{\mu}_1(a)$; 4) $\vec{\mu}_2(d)$ to $\vec{\mu}_2(a)$;

where the indices 1 and 2 refer to the two tautomeric forms of a FbP unit.

From the optimised geometry of **2**, and using eq.(S3), one obtains:

$$\kappa_{11}=1.30, \kappa_{12}=1.21; \kappa_{21}=0 \text{ and } \kappa_{22}=0.48.$$

With $|\vec{\mu}_1|=|\vec{\mu}_2|=2.20 \text{ D}^{\text{S4}}$ and $r_{da}=1.17 \text{ nm}$, one gets:

$|V_{11}|=20.5 \text{ cm}^{-1}$; $|V_{12}|=19.1 \text{ cm}^{-1}$; $|V_{21}|=0 \text{ cm}^{-1}$, and $|V_{22}|=7.6 \text{ cm}^{-1}$.

Finally with : $\Theta=3.7 \cdot 10^{-5} \text{ cm}^{\text{S4}}$ the EEH rate constants are:

$k_{11}=1.83 \cdot 10^{-2} \text{ ps}^{-1}$; $k_{12}=1.60 \cdot 10^{-2} \text{ ps}^{-1}$; $k_{21}=0 \text{ ps}^{-1}$, and $k_{22}=2.5 \cdot 10^{-3} \text{ ps}^{-1}$;

The average gives the EEH rate constant in **2**: $k_{\text{EEH}}=(109 \text{ ps})^{-1}$.

- S1. X. Gao, W. Qiu, X. Yang, Y. Liu, Y. Wang, H. Zhang, T. Qi, Y. Liu, K. Lu, C. Du, Z. Shuai, G. Yu and D. Zhu, *Org. Lett.*, 2007, **9**, 3917-3920.
- S2. R. Luguya, L. Jaquinod, F. R. Fronczek, M. G. H. Vicente and K. M. Smith, *Tetrahedron*, 2004, **60**, 2757-2763.
- S3. T. Pullerits, S. Hess, J. L. Herek and V. Sundström, *J. Phys. Chem. B*, 1997, **101**, 10560-10567.
- S4. D. Villamaina, S. Bhosale, S. J. Langford and E. Vauthey, *Phys. Chem. Chem. Phys.*, 2013, **15**, 1177-1187.